

Effect of magnetic field on wave propagation in cylindrical poroelastic bone with cavity

A.M. Farhan^{*1,2}

¹Physics Department, Faculty of Science, Jazan University, Jazan, Saudi Arabia

²Physics Department, Faculty of Science, Zagazig University, Zagazig, Egypt

(Received April 29, 2016, Revised December 26, 2016, Accepted January 9, 2017)

Abstract. In this paper, the wave propagation in an infinite poroelastic cylindrical bone with cavity is studied. An exact closed form solution is presented by employing an analytical procedure. The frequency equation for poroelastic bone is obtained when the boundaries are stress free and is examined numerically. The magnitude of the frequency equation, wave velocity and attenuation coefficient are calculated for poroelastic bone for different values of magnetic field, density and frequency. In wet bone little frequency dispersion was observed, in contrast to the results of earlier studies. Such a model would in particular be useful in large-scale parametric studies of bone mechanical response. Comparison was made with the results obtained in the presence and absence of magnetic field. The results indicate that the effect of magnetic field, density and frequency on wave propagation in poroelastic bone are very pronounced.

Keywords: wave propagation; poroelastic; wet bone; magnetic field; natural frequency

1. Introduction

The study of wave propagation over a continuous media is of practical importance in the field of engineering, medicine and in bio-engineering. Application of the poroelastic materials in medical fields such as orthopaedics, dental and cardiovascular is well known. In orthopaedics, wave propagation over bone is used in monitoring the rate of fracture healing. There are two types of osseous tissue such as cancellous or trabecular and compact or cortical bone, which are of different materials, with respect to their mechanical behavior. In macroscopic terms the percentage of porosity in the cortical bone is 3-5%, whereas in the trabecular or cancellous the percentage of porosity is up to 90% (Natal and Meroi 1986). The extensive literature on the topic is now available and we can only mention a few recent interesting investigations in (Ahmed and Abd-Alla 2002, El-Naggar *et al.* 2001, Abd-Alla *et al.* 2011, Abd-Alla and Abo-Dahab 2013, Abo-Dahab *et al.* 2014, Abd-Alla and Yahia 2013). Cardoso and Cowin (2012) investigated the role of structural anisotropy of biological tissues in poroelastic wave propagation. Wen (2010) studied the solution of coupled poroelastic/acoustic/elastic wave propagation problems using automatic *hp*-adaptivity. Morin and Hellmich (2014) presented a multiscale poromicromechanical approach to wave propagation and attenuation in bone. Potsika *et al.* (2014) in his analysis has studied application of an effective medium theory for modelling ultrasound wave propagation in healing long bones. Papathanasopoulou *et al.* (2002) investigated a

poroelastic bone model for internal remodeling. Nguyen *et al.* (2010) considered poroelastic behaviour of cortical bone under harmonic axial loading: A finite element study at the osteonal scale. Misra and Samanta (1984) investigated the wave propagation in tubular bones. Qin *et al.* (2005) studied the thermoelectroelastic solutions for surface bone remodeling under axial and transverse loads. Mathieu *et al.* (2014) presented the biomechanical determinants of the stability of dental implants: Influence of the bone-implant interface properties. Brynk *et al.* (2011) in his analysis has studied the experimental poromechanics of trabecular bone strength: Role of Terzaghi's effective stress and of tissue level stress fluctuations. Analytical methods to determine the effective mesoscopic and macroscopic elastic properties of cortical bone was studied by Parnell *et al.* (2012). Shah (2011) investigated the flexural wave propagation in coated poroelastic cylinders with reference to fretting fatigue. Gilbert *et al.* (2012) studied the quantitative ultrasound model of the bone with blood as the interstitial fluid. Cui *et al.* (1997) discussed the poroelastic solutions of an inclined borehole. Cowin (1999) studied the bone poroelasticity. Mathieu *et al.* (2012) studied the influence of Healing Time on. The ultrasonic response of the bone-Implant Interface. Misra (1994) investigated the thermo-viscoelastic waves in an infinite aeolo-tropic body with a cylindrical cavity a study under the review of generalized theory of thermoelasticity. Shah (2008) presented the axially symmetric vibrations of fluid-filled poroelastic circular cylindrical shells. The extensive literature on the topic is now available and we can only mention a few recent interesting investigations in refs. (Tounsi 2013, Boudierba *et al.* 2013, Belabed *et al.* 2014, Zidi *et al.* 2014, Meziane *et al.* 2014, Fi *et al.* 2014, Hebali *et al.* 2013, 2014, Fekrar *et al.* 2014, Akbarov *et al.* 2015, Marin *et al.* 2015, Abo-Dahab *et al.* 2016, Abd-Alla *et al.* 2015, Kumar *et al.* 2016,

*Corresponding author, Professor
E-mail: afarhan_afarhan@yahoo.com

Said and Othman 2016, Bakora and Tounsi 2015).

In the present analysis, the frequency equation for the system considered is obtained when the lateral surface is stress free. The frequencies are calculated for poroelastic bone is obtained for various values of magnetic field are given in graphs. The propagation of flexural waves in an infinite cylindrical bone element which is porous in nature is being considered and numerical results are carried out. Our results are presented for various parameters of elastic bone. The results indicate that the effect of magnetic field is very pronounced.

2. Formulation of the problem

Modeling on the concept of the Biot (1995, 1996) the constitutive equations for a transversely isotropic case with z as axis of the symmetry are taken in polar coordinates as

$$\begin{aligned} \tau_{rr} &= c_{11} \frac{\partial u_r}{\partial r} + c_{12} r^{-1} \left(u_r + \frac{\partial u_\theta}{\partial \theta} \right) + c_{13} \frac{\partial u_z}{\partial z}, \\ &+ M \left[\frac{\partial v_r}{\partial r} + r^{-1} \left(v_r + \frac{\partial v_\theta}{\partial \theta} \right) + \frac{\partial v_z}{\partial z} \right] \\ \tau_{\theta\theta} &= c_{12} \frac{\partial u_r}{\partial r} + c_{11} r^{-1} \left(u_r + \frac{\partial u_\theta}{\partial \theta} \right) + c_{13} \frac{\partial u_z}{\partial z}, \\ &+ M \left[\frac{\partial v_r}{\partial r} + r^{-1} \left(v_r + \frac{\partial v_\theta}{\partial \theta} \right) + \frac{\partial v_z}{\partial z} \right] \\ \tau_{zz} &= c_{13} \left[\frac{\partial u_r}{\partial r} + r^{-1} \left(u_r + \frac{\partial u_\theta}{\partial \theta} \right) \right] + c_{33} \frac{\partial u_z}{\partial z} \\ &+ Q \left[\frac{\partial v_r}{\partial r} + r^{-1} \left(v_r + \frac{\partial v_\theta}{\partial \theta} \right) + \frac{\partial v_z}{\partial z} \right], \\ \tau_{rz} &= c_{44} \left[\frac{\partial u_z}{\partial r} + \frac{\partial u_r}{\partial z} \right], \\ \tau_{r\theta} &= c_{66} \left[\frac{\partial u_\theta}{\partial r} + r^{-1} \left(\frac{\partial u_r}{\partial \theta} - u_\theta \right) \right] \\ \tau_{\theta z} &= c_{44} \left[\frac{\partial u_\theta}{\partial z} + r^{-1} \frac{\partial u_z}{\partial \theta} \right] \end{aligned} \tag{1}$$

$$\begin{aligned} \tau &= M \left[\frac{\partial u_r}{\partial r} + r^{-1} \left(u_r + \frac{\partial u_\theta}{\partial \theta} \right) \right] + Q \frac{\partial v_z}{\partial z} \\ &+ R \left[\frac{\partial v_r}{\partial r} + r^{-1} \left(v_r + \frac{\partial v_\theta}{\partial \theta} \right) + \frac{\partial v_z}{\partial z} \right], \end{aligned} \tag{2}$$

$$\sigma_{rr} = \mu_e H^2 \left(\frac{\partial^2 u_r}{\partial r^2} + \frac{1}{r} \frac{\partial u_r}{\partial r} + \frac{1}{r} \frac{\partial u_z}{\partial z} + \frac{\partial^2 u_z}{\partial r \partial z} + \frac{1}{r^2} \frac{\partial^2 u_r}{\partial r \partial \theta} \right) \tag{2a}$$

$$\sigma_{zz} = \mu_e H^2 \left(\frac{\partial u_r}{\partial r} + \frac{1}{r} u_r + \frac{\partial u_z}{\partial z} \right) \tag{2b}$$

where τ_{ij} and τ are the average stresses of solid and fluid respectively and σ_{rr} , σ_{zz} are the magnetic stresses, with elastic constant c_{ij} , M , Q , R , $c_{66}=(c_{11}-c_{12})/2$ and H is the magnetic field

The equation of the flow is

$$b_{rr}^{-1} \nabla^2 \tau + b_{zz}^{-1} \tau_{zz} = \frac{\partial(\varepsilon - \tau)}{\partial t}, \tag{3}$$

$$e_{ij} = \left(\frac{1}{2} \right) (u_{i,j} + u_{j,i}) \tag{4}$$

where $b_{rr} = \mu f^2 / k_{rr}$, $b_{zz} = \mu f^2 / k_{zz}$, ∇^2 is Laplacian operator in polar coordinates, μ is the viscosity, f is the porosity, k_{rr} , k_{zz} are the permeability of the medium. The

average displacements of solid and velocity of fluid phases are taken as u_i and v_i respectively.

The strains are expressed as and dilation of the phases as

$$e = u_{i,j} \text{ and } \varepsilon = V_{i,i} \quad (i, j = r, \theta, z) \tag{5}$$

The equation of motion with magnetic field are

$$\begin{aligned} &\frac{\partial \tau_{rr}}{\partial r} + r^{-1} \frac{\partial \tau_{r\theta}}{\partial \theta} + \frac{\partial \tau_{rz}}{\partial z} + r^{-1} (\tau_{rr} - \tau_{\theta\theta}) + \\ &\mu_e H^2 \left(\frac{\partial^2 u_r}{\partial r^2} + \frac{1}{r} \frac{\partial u_r}{\partial r} + \frac{1}{r} \frac{\partial u_z}{\partial z} + \frac{\partial^2 u_z}{\partial r \partial z} + \frac{1}{r^2} \frac{\partial^2 u_r}{\partial r \partial \theta} \right) \\ &= \rho \frac{\partial^2 u_r}{\partial t^2} \\ &\frac{\partial \tau_{rz}}{\partial r} + r^{-1} \frac{\partial \tau_{\theta z}}{\partial \theta} + \frac{\partial \tau_{zz}}{\partial z} + r^{-1} \tau_{rz} + \\ &\mu_e H^2 \left(\frac{1}{r^2} \frac{\partial^2 u_z}{\partial \theta^2} + \frac{\partial^2 u_r}{\partial r \partial z} + \frac{\partial^2 u_z}{\partial z^2} \right) \\ &= \rho \frac{\partial^2 u_r}{\partial t^2} \\ &\frac{\partial \tau_{r\theta}}{\partial r} + r^{-1} \frac{\partial \tau_{\theta\theta}}{\partial \theta} + \frac{\partial \tau_{\theta z}}{\partial z} + 2r^{-1} \tau_{\theta r} \\ &= \rho \frac{\partial^2 u_\theta}{\partial t^2} \end{aligned} \tag{6}$$

where ρ is the density of the bone, μ_e is the magnetic permeability coefficient and t is the time.

Substituting from Eq. (1) into Eq. (6), we obtain

$$\begin{aligned} &(c_{11} + \mu_e H^2 \left[\frac{\partial^2 u_r}{\partial r^2} + r^{-1} \frac{\partial u_r}{\partial r} + \frac{1}{r^2} \frac{\partial^2 u_r}{\partial r \partial \theta} \right] + r^{-2} \frac{1}{2} (c_{11} \\ &- c_{12}) \frac{\partial^2 u_r}{\partial \theta^2} + r^{-1} \left(\frac{1}{2} (c_{12} - c_{11}) \right) \frac{\partial^2 u_\theta}{\partial \theta \partial r} \\ &- r^{-2} \left(\frac{3}{2} (c_{11} - c_{12}) \right) \frac{\partial u_\theta}{\partial \theta} - c_{11} \frac{1}{r^2} u_r \\ &+ (c_{13} + c_{44} + \mu_e H^2) \frac{\partial^2 u_z}{\partial r \partial z} + \mu_e H^2 \frac{1}{r} \frac{\partial u_z}{\partial z} \\ &+ M \left[\frac{\partial^2 v_r}{\partial r^2} + r^{-1} \frac{\partial v_r}{\partial r} - r^{-2} v_r - r^{-2} \frac{\partial^2 v_\theta}{\partial \theta^2} \right. \\ &\left. + \frac{\partial^2 v_z}{\partial r \partial z} \right] = \rho \frac{\partial^2 u_r}{\partial t^2}, \\ &r^{-1} \left(\frac{1}{2} (c_{11} + c_{12}) \right) \frac{\partial^2 u_r}{\partial \theta \partial r} + r^{-2} \left(\frac{3}{2} (c_{11} - c_{12}) \right) \frac{\partial u_r}{\partial \theta} \\ &+ \frac{1}{2} (c_{11} - c_{12}) \left[\frac{\partial^2 u_\theta}{\partial r^2} + r^{-1} \frac{\partial u_\theta}{\partial r} - r^{-2} u_\theta \right] + r^{-2} c_{11} \frac{\partial^2 u_\theta}{\partial \theta^2} \\ &+ c_{44} \frac{\partial^2 u_\theta}{\partial z^2} + r^{-1} (c_{13} + c_{44}) \frac{\partial^2 u_z}{\partial \theta \partial z} \\ &+ r^{-1} M \left[\frac{\partial^2 v_r}{\partial r \partial \theta} + r^{-1} \frac{\partial v_r}{\partial \theta} + r^{-1} \frac{\partial^2 v_\theta}{\partial \theta^2} + \frac{\partial^2 v_z}{\partial r \partial z} \right] = \rho \frac{\partial^2 u_\theta}{\partial t^2}, \end{aligned}$$

$$\begin{aligned}
 & (c_{13} + c_{44} + \mu_e H^2) \frac{\partial^2 u_r}{\partial r \partial z} + r^{-1}(c_{13} + c_{44}) \frac{\partial u_r}{\partial z} \\
 & + r^{-1}(c_{13} + c_{44}) \frac{\partial^2 u_\theta}{\partial \theta \partial z} + (c_{44} + \mu_e H^2) \\
 & \left[\frac{\partial^2 u_z}{\partial r^2} + r^{-1} \frac{\partial u_z}{\partial r} - r^{-2} \frac{\partial^2 u_z}{\partial \theta^2} \right] + (c_{44} + \mu_e H^2) \frac{\partial^2 u_z}{\partial z^2} \\
 & + Q \left[\frac{\partial^2 v_r}{\partial r \partial z} + r^{-1} \frac{\partial v_r}{\partial z} + r^{-1} \frac{\partial^2 v_\theta}{\partial \theta \partial z} + \frac{\partial^2 v_z}{\partial z^2} \right] = \rho \frac{\partial^2 u_z}{\partial t^2}. \quad (7)
 \end{aligned}$$

3. Solution of the problem

We seek the solution in the form

$$\begin{aligned}
 u_r(r, \theta, z, t) &= \left[\frac{\partial \Phi}{\partial r} + \frac{1}{r} \frac{\partial \Psi}{\partial \theta} \right] e^{i(kz - \omega t)}, \\
 v_r(r, \theta, z, t) &= -\frac{\partial \eta}{\partial r} e^{i(kz - \omega t)}, \\
 u_\theta(r, \theta, z, t) &= \left[\frac{1}{r} \frac{\partial \Phi}{\partial \theta} - \frac{\partial \Psi}{\partial r} \right] e^{i(kz - \omega t)}, \\
 v_\theta(r, \theta, z, t) &= -\frac{1}{r} \frac{\partial \eta}{\partial \theta} e^{i(kz - \omega t)}, \\
 u_z(r, \theta, z, t) &= \left[\frac{i}{h} W \right] e^{i(kz - \omega t)}, \\
 v_z(r, \theta, z, t) &= -ik\eta e^{i(kz - \omega t)}, \quad (8)
 \end{aligned}$$

where, $u_r, u_\theta, u_z, v_r, v_\theta$ and v_z are mechanical displacements and velocities, ω is the angular frequency, k is the wave number and thickness of the cylinder $h=b-a$ where a is the inner radius, b is the outer radius and Φ, Ψ, w, η are functions of r and θ .

Substituting from Eq. (8) into Eq. (7), the following equations are obtained

$$\begin{aligned}
 & ((c_{11} + \mu_e H^2) \nabla^2 + \rho \omega^2 - k^2(c_{44} - \mu_e H^2)) \Phi \\
 & - (c_{13} + c_{44} + \mu_e H^2) \left(\frac{k\zeta}{h} \right) - M(\nabla^2 - k^2)\eta = 0 \\
 & ((c_{44} + \mu_e H^2) \nabla^2 + \rho \omega^2 - k^2 c_{33}) \left(\frac{\zeta}{h} \right) \\
 & + (c_{13} + c_{44} + \mu_e H^2) k \nabla^2 \Phi - kQ(\nabla^2 - k^2)\eta = 0, \\
 & \left\{ M \left[\frac{\nabla^4}{b rr} - \frac{k^2 \nabla^2}{b_{zz}} \right] + i\omega \nabla^2 \right\} \Phi \\
 & + \left\{ \left(\frac{Q}{h} \right) \left[\frac{-k \nabla^2}{b rr} + \frac{k^3}{b_{zz}} \right] - \frac{ik\omega}{h} \right\} \zeta \\
 & + \left\{ R \left[\frac{-\nabla^2(\nabla^2 - k^2)}{b rr} + \frac{k^2(\nabla^2 - k^2)}{b_{zz}} \right] i\omega(\nabla^2 - k^2) \right\} \eta = 0 \\
 & \left(\frac{1}{2}(c_{11} + \mu_e H^2) - c_{12} \right) \nabla^2 + \rho \omega^2 - k^2(c_{44} - \mu_e H^2) \\
 & \psi = 0 \quad (9)
 \end{aligned}$$

$$\begin{aligned}
 & \nabla^2(\nabla^2 - b\varepsilon 1^2 + iD)\Phi - \varepsilon 1(Q'\nabla^2 + bQ'\varepsilon 1^2 - iD)\zeta \\
 & + (-R'\nabla^2 + bR'\varepsilon 1^2 + iD)\xi = 0, \quad (10)
 \end{aligned}$$

$$(c_{66} \nabla^2 + (ch)^2 - \varepsilon 1^2)\Psi = 0, \quad (11)$$

where

$$\begin{aligned}
 \xi &= (\nabla^2 - k^2)\eta, D = \frac{\omega h^2 b_{rr}}{M}, Q' = \frac{Q}{M}, \\
 R' &= \frac{R}{M}, \bar{M} = \frac{M}{c_{44} + \mu_e H^2},
 \end{aligned}$$

$$\begin{aligned}
 \bar{Q} &= \frac{Q}{c_{44} + \mu_e H^2}, c^2 = \frac{\rho \omega^2}{c_{44} + \mu_e H^2}, \\
 b &= \frac{b_{rr}}{b_{zz}}, \bar{c}_{ij} = \frac{c_{ij}}{c_{44}} \quad (i, j = 1, 2, 3),
 \end{aligned}$$

By defining the dimensionless coordinate $r = \frac{r}{h}$ and $\varepsilon 1 = kh$, the above equations are written in dimensionless parameter r and $\varepsilon 1$ as

$$\begin{aligned}
 & ((c_{11} + \mu_e H^2) \nabla^2 + (ch)^2 - \varepsilon 1^2) \Phi \\
 & - (c_{13} + 1)(\varepsilon 1 \zeta) - \bar{M} \xi = 0, \\
 & (\nabla^2 + (ch)^2 - \varepsilon 1^2 c_{33}) \zeta + (c_{13} + 1) \varepsilon 1 \nabla^2 \Phi - \varepsilon 1 \bar{Q} \xi = 0, \\
 & \nabla^2 = \frac{\partial^2}{\partial r^2} + \frac{1}{r} \frac{\partial}{\partial r} + \frac{1}{r^2} \frac{\partial^2}{\partial \theta^2} \quad (12)
 \end{aligned}$$

The reason for ξ begin defined as above and not being solved for the variable η is that the flow of fluid through the boundaries of bone does not take place during the study of the propagation of waves. However η can be calculated if the flow on the boundaries are prescribed. Writing Eq. (10) in the determinant form

$$\begin{vmatrix}
 ((c_{11} + \mu_e H^2) \nabla^2 + A) & -B & -\bar{M} \\
 B \nabla^2 & (\nabla^2 + C) & -\bar{Q} \varepsilon 1 \\
 T_1 & T_2 & T_3
 \end{vmatrix} (\Phi, \zeta, \xi) = 0, \quad (13)$$

Where

$$\begin{aligned}
 T_1 &= \nabla^2(\nabla^2 - b\varepsilon 1^2 + iD), \\
 T_2 &= -\varepsilon 1(Q'\nabla^2 + bQ'\varepsilon 1^2 - iD), \\
 T_3 &= (-R'\nabla^2 + bR'\varepsilon 1^2 + iD), A = (ch)^2 - \varepsilon 1^2, \\
 \bar{B} &= (1 + \bar{c}_{13}) \varepsilon 1 \text{ and } C = (ch)^2 - \varepsilon 1^2 \bar{c}_{33}.
 \end{aligned}$$

Evaluating the determinant form, the following equations are obtained

$$(\nabla^6 + P\nabla^4 + G\nabla^2 + T)(\Phi, \zeta, \xi) = 0, \quad (14)$$

where

$$\begin{aligned}
 P &= (R'\varepsilon 1^2(\bar{c}_{11} + \mu_e H^2) + iD(\bar{c}_{11} + \mu_e H^2) + cR'(\bar{c}_{11} + \mu_e H^2) \\
 & - \bar{Q}Q'\varepsilon 1^2(\bar{c}_{11} + \mu_e H^2)AR' - B^2R' + BQ'\varepsilon 1 + \bar{M}\varepsilon 1^2 \\
 & - \bar{Q}\varepsilon 1B + i\bar{M}D + \bar{M}D)/(-R'(\bar{c}_{11} + \mu_e H^2) + \bar{M}),
 \end{aligned}$$

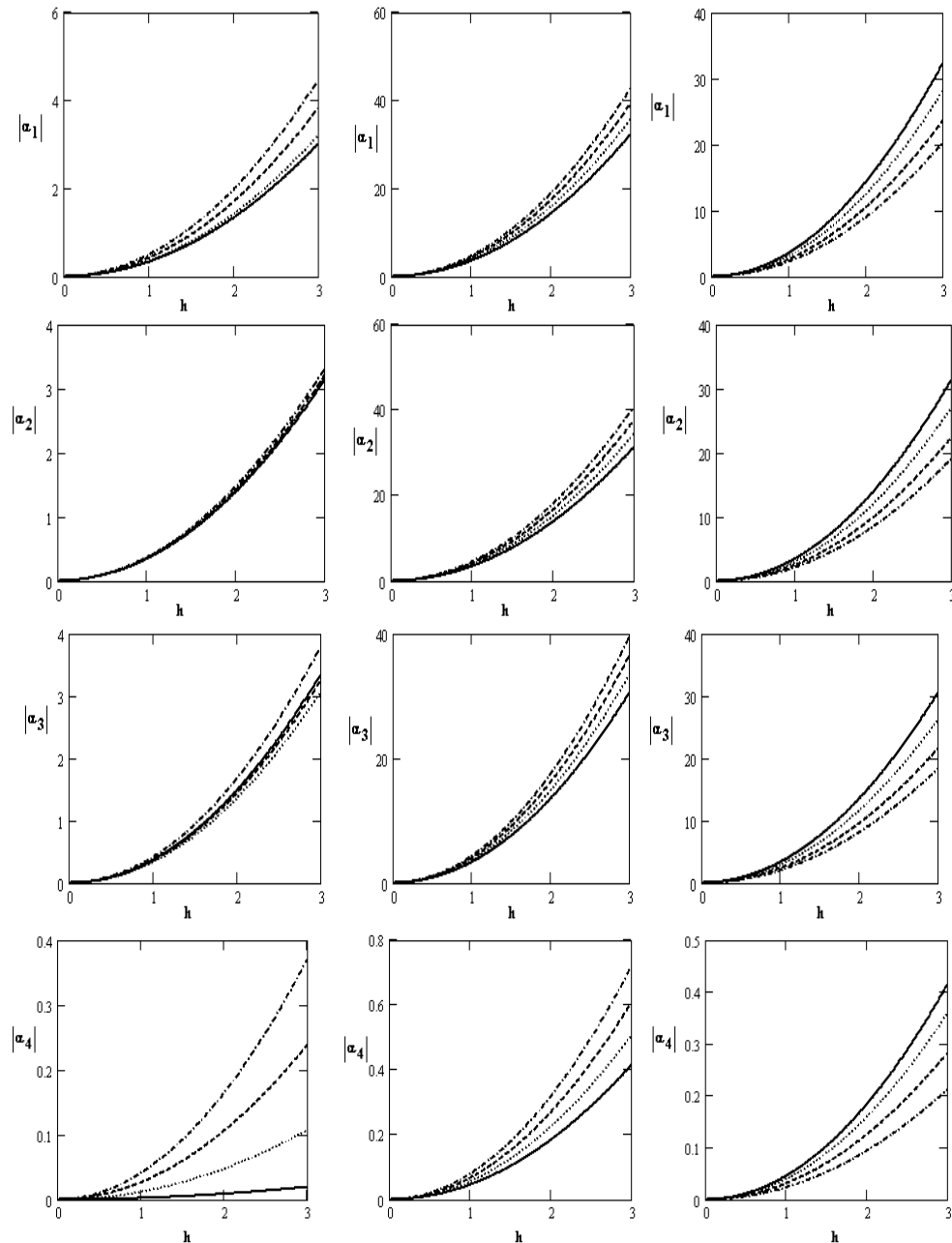
$G =$

$$\begin{aligned}
 & (CR'\varepsilon 1^2(\bar{c}_{11} + \mu_e H^2) + iDC(\bar{c}_{11} + \mu_e H^2) \\
 & + Q'\varepsilon 1^4\bar{Q}(\bar{c}_{11} + \mu_e H^2) - iD\bar{Q}\varepsilon 1^2(\bar{c}_{11} + \mu_e H^2) \\
 & + AR'\varepsilon 1^2 + iDA + AR'C - AQ'\bar{Q}\varepsilon 1^2 + BD\varepsilon 1^3 \\
 & - iD\varepsilon 1 + C\varepsilon 1^2 - B\bar{Q}\varepsilon 1^3 + iDB\varepsilon 1\bar{M} + iDC\bar{M} - \bar{M}C\varepsilon 1^2) \\
 & /(-R'(\bar{c}_{11} + \mu_e H^2) + \bar{M})
 \end{aligned}$$

$$T = \frac{A(CR'\varepsilon 1^2 + iDC + \bar{Q}Q'\varepsilon 1^4 - iD\bar{Q}\varepsilon 1^2)}{-R'(\bar{c}_{11} + \mu_e H^2) + \bar{M}}.$$

The solution of Eq. (14) can be written as

$$\begin{aligned}
 \Phi &= \sum_{i=1}^3 [A_i J_n(\alpha_i x) + B_i Y_n(\alpha_i x)] \cos(n\theta), \\
 \zeta &= \sum_{i=1}^3 d_i [A_i J_n(\alpha_i x) + B_i Y_n(\alpha_i x)] \cos(n\theta),
 \end{aligned}$$



$\rho = 1 \text{---}, 3 \dots, 6 \text{--}, 9 \text{..}$ $\omega = 1 \text{--}, 1.1 \dots, 1.2 \text{--}, 1.3 \text{..}$ $H = 0.1 \text{--}, 0.3 \dots, 0.5 \text{--}, 0.7 \text{..}$
 Fig. 1 Variations of the roots $|\alpha_j|$ ($j=1,2,3,4$) with respect to the thickness h with the variation

$$\xi = \sum_{i=1}^3 e_i [A_i J_n(\alpha_i x) + B_i Y_n(\alpha_i x)] \cos(n\theta), \quad (15)$$

where α_i^2 are the non-zero roots of the equation and $J_n(\cdot)$, $Y_n(\cdot)$ are Bessel's functions of first and second kind of order n respectively

$$\begin{aligned} \alpha^6 - P\alpha^4 + G\alpha^2 - H &= 0, \\ \alpha_1^2 &= \frac{P}{3} - \frac{\sqrt[3]{2}(3G - P^2)}{3F1} + \frac{F1}{3\sqrt[3]{2}}, \\ \alpha_2^2 &= \frac{P}{3} + \frac{(1+i\sqrt{3})(3G - P^2)}{\sqrt[3]{32}F1} - \frac{(1-i\sqrt{3})F1}{\sqrt[3]{62}}, \\ \alpha_3^2 &= \frac{P}{3} + \frac{(1-i\sqrt{3})(3G - P^2)}{\sqrt[3]{1024}F1} - \frac{(1+i\sqrt{3})F1}{\sqrt[3]{62}}. \end{aligned} \quad (16)$$

Where

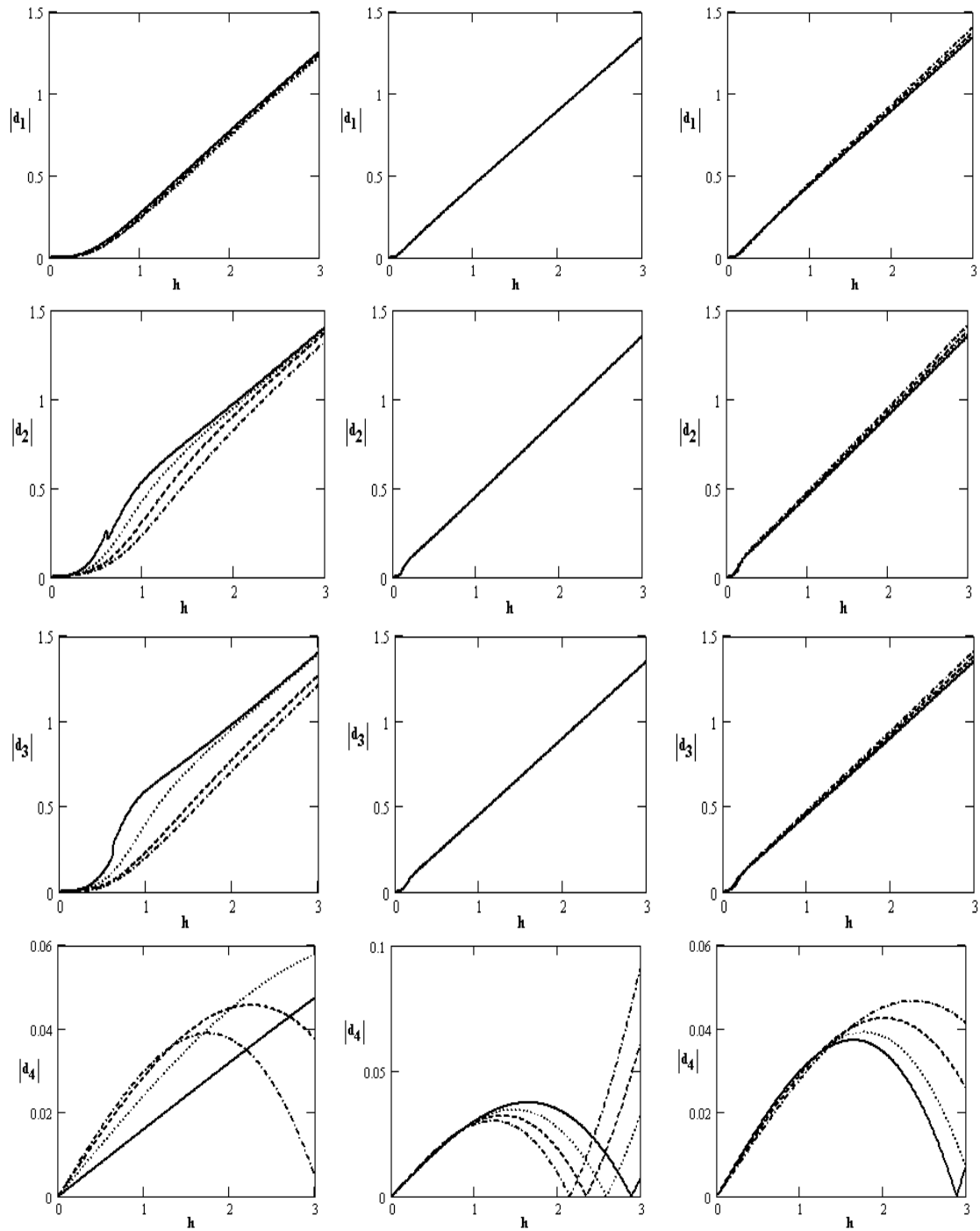
$$F1 = (27T - 9GP + 2P^3 + 3\sqrt{3}\sqrt{4G^3 + 27T^2 - 18GTP + 4TP^3})^{\frac{1}{3}}$$

and d_i and e_i are given by

$$\begin{aligned} ((1 + \bar{c}_{13})\epsilon_1 d_i + \bar{M}e_i &= (\bar{c}_{11} + \mu_e H^2)\alpha_i^2 - (ch)^2 - \epsilon_1^2), \\ (-\alpha_i^2 + (ch)^2 - \epsilon_1^2 \bar{c}_{33})d_i - \bar{Q}\epsilon_1 e_i &= (1 + \bar{c}_{13})\epsilon_1 \alpha_i^2. \end{aligned} \quad (17)$$

Solving Eq. (11) we have

$$\Psi = [A_4 J_n(\alpha_4 x) + B_4 Y_n(\alpha_4 x)] \sin(n\theta), \quad (18)$$



$\rho = 1 \text{---}, 3 \dots, 6 \text{---}, 9 \text{---}$ $\omega = 1 \text{---}, 1.1 \dots, 1.2 \text{---}, 1.3 \text{---}$ $H = 0.1 \text{---}, 0.3 \dots, 0.5 \text{---}, 0.7 \text{---}$

Fig. 2 Variations of $|d_j|$ ($j=1,2,3,4$) with respect to the thickness h with the variation of ρ , ω and H

where

$$\alpha_4^2 = \frac{2((ch)^2 - \epsilon 1^2)}{(\bar{c}_{11} - \bar{c}_{12} + H^2)}$$

$$\begin{aligned} \tau_{rr} + \sigma_{rr} = \tau_{rz} = \tau_{r\theta} = \tau = 0 \text{ at } r = \bar{a}, \\ \tau_{rr} + \sigma_{rr} = \tau_{rz} = \tau_{r\theta} = \tau = 0 \text{ at } r = \bar{b}, \end{aligned} \quad (19)$$

where $\bar{a} = \frac{a}{h}$, $\bar{b} = \frac{b}{h}$

Using Eqs. (8), (15), (18) in (19), we obtain frequency equation in the form

$$|a_{ij}| = 0 \quad (i, j = 1, 2, 3, \dots, 8), \quad (20)$$

where, the coefficients of a_{ij} are take the form in

4. Boundary conditions and the frequency equation

For the vibration, the mechanical boundary conditions are

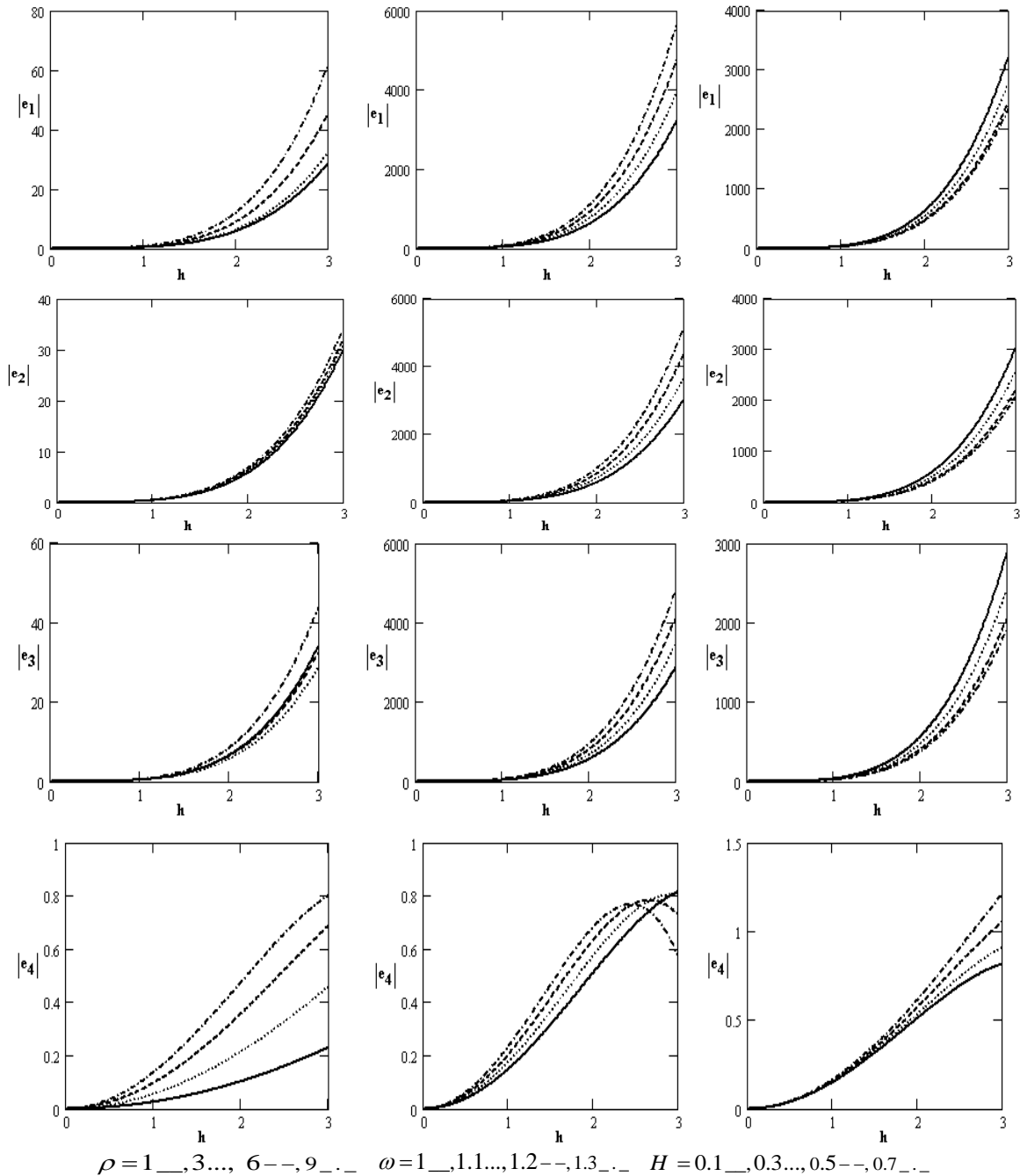


Fig. 3 Variations of $|e_j|$ ($j=1,2,3,4$) with respect to the thickness h with the variation of ρ , ω and H

Appendix A in the paper end.

Eq. (20) is a transcendental equation of the frequency and wave number. The roots of Eq. (20) provide the dispersion curves of the guided modes. i.e., the wave number as a function of frequency

5. Numerical results and discussion

The numerical results for the frequency equation are computed for the bone. Since the frequency equation is transcendental in nature, there are an infinite number of roots for the frequency equation. The results are evaluated

in the $0 < \varepsilon l < 4$ and $0 < ch < 4$ with the ratio $b/a=3.0$. The values of the elastic constant of the bone are taken from Ahmed and Abd-Alla (2002) and the poroelastic constant is evaluated from the expression given by Davis Sr (1970), i.e.

$$Q = (1 - f - \frac{\delta}{\chi}) / (\gamma + \delta + (\delta^2 / \chi)),$$

$$R = f^2 / (\gamma + \delta + (\delta^2 / \chi))$$

where f is the porosity and γ , δ , χ are given by Young's modulus and the Poisson ratio. The expression for γ , δ , χ are given by $\chi=3(1-2\nu)/E$, $\delta=0.6\chi$ and $\gamma=f(c-\delta)$ where c is taken to be zero for incompressibility of the fluid.

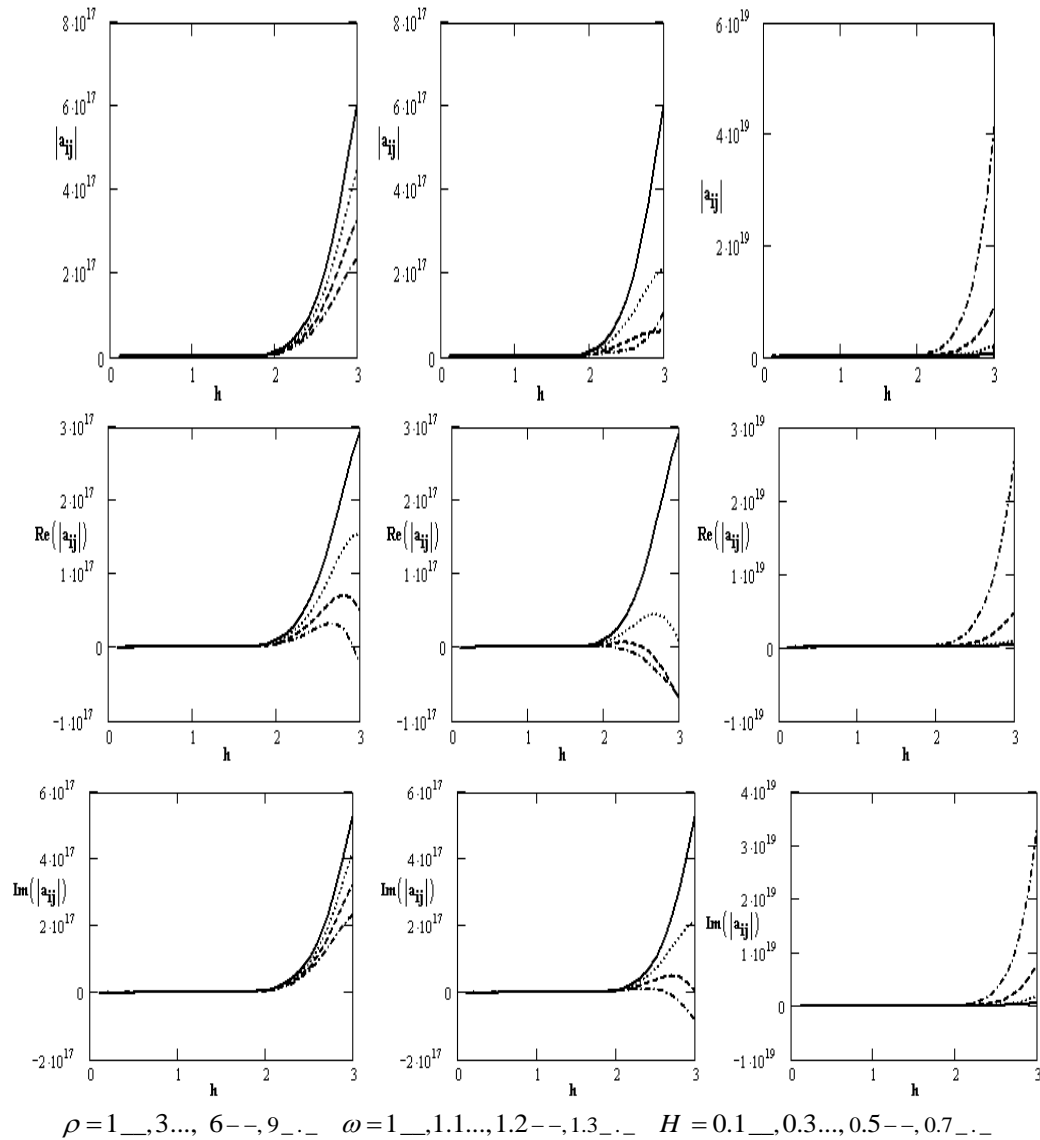


Fig. 4 Variations of $|a_{ij}|$, $\text{Re}(a_{ij})$, $\text{Im}(a_{ij})$ with respect to the thickness h with the variation of ρ , ω and H

The porosity of the human bone in the age group 35-40 years is taken to be 0.24 (Ghista 1979). In order to evaluate one more poroelastic constant it is assumed that $M/Q \cong c_{12}/c_{13}$ as the value M is not provided. Since the fluid in general is isotropic, it is taken that $b_{rr} = b_{zz}$. The density of the fluid in the porospace, permeability of the medium and mass density of the bone are taken from Ahmed and Abd-Alla (2002).

The magnitude of the frequency equation $|a_{ij}|$, wave velocity $\text{Re}(a_{ij})$ and attenuation coefficient $\text{Im}(a_{ij})$, we now numerical results by using bi-section method for different density ρ , the angular velocity ω and magnetic field H . The numerical work has been carried out with the help of computer programming using the software Matlab.

Fig. 1 shows the coefficients of a_1 , a_2 , a_3 and a_4 for poroelastic bone with respect to the thickness h for different values of density ρ , the angular velocity ω and magnetic field H , which it increases as the thickness increases, while it increases with increasing of the density, frequency and magnetic field, except when effect of the density, as well,

the coefficient of a_3 increases and decreases as the density increases.

Fig. 2 shows the coefficients of $|d_1|$, $|d_2|$, $|d_3|$ and $|d_4|$ for poroelastic bone with respect to the thickness h for different values of density ρ , the angular velocity ω and magnetic field H , which it increases with increasing of thickness, while it increases with increasing of density, as well there is no effect of density, frequency and magnetic field on coefficients $|d_1|$, $|d_2|$, $|d_3|$. It is obvious that the coefficient $|d_4|$ decreases as the frequency and magnetic field increase while it increases as the density increase, which it has oscillatory behavior in the whole range of the h -axis for different values of the density, frequency and magnetic field.

Fig. 3 shows the variations of the coefficients for poroelastic bone of e_1 , e_2 , e_3 and e_4 with respect to the thickness h for different values of density ρ , the angular velocity ω and magnetic field H , which it increases with increasing of the thickness, while it increases as the density, frequency and magnetic field increase, as well $|e_3|$ increases

Table 1 Summarizes the approximate geometry of the femur and the material constants which are used in the computations Ahmed and Abd-Alla (2002)

| c_{11} | c_{12} | c_{13} | c_{33} | c_{44} | a | b |
|----------|----------|----------|----------|----------|-----|-----|
| 2.12 | 0.95 | 1.02 | 3.76 | 0.75 | 0.8 | 1.4 |

and decreases when effect of density, while $|e_4|$ has oscillatory behavior in the whole range of the h -axis for different values of frequency and magnetic field.

Fig. 4 show the variations of the magnitude of the frequency equation $|a_{ij}|$, wave velocity $\text{Re}(a_{ij})$ and attenuation coefficient $\text{Im}(a_{ij})$ with respect to the thickness h for different values of density ρ , frequency ω and magnetic field H , which it coincides on the interval $[0,2]$, while it has oscillatory behavior for $h > 2$. It is notice that the magnitude of the frequency equation, wave velocity and attenuation decrease with increasing of density and frequency for $h > 2$, while it increases as the magnetic field increases.

6. Conclusions

In this paper, the wave propagation of poroelastic bone with circular cylinder subjected to traction free surfaces is considered. We adopted the analysis of [3], and the solution of the problem was expressed in terms of a Bessel function of the first and second kind, respectively.

The resulting frequency equation has been solved numerically. The contribution of the fluid term to wave propagation is a well-established possible mechanism of wave propagation connected to many biological phenomena observed in bone. Although the prediction of the model cannot be trusted quantitatively at this stage, its qualitative behavior complies with the predictions of other theoretical and experimental models referred to in the literature. Acalibration of the model and its verification with experimental data is in progress. Important phenomena are observed in all these computations as follows:

(i) The frequency equation of axial symmetric vibrations is independent of the nature of the surface, magnetic field, and the presence of fluid in the poroelastic cylindrical.

(ii) By comparing Figs. 1-4, it was found that the frequency equation, phase velocity, and attenuation coefficient have the same behaviour in both media; but, with the passage of magnetic field, frequency, density and thickness, numerical values of frequency in the poroelastic cylinder are large in comparison due to the influences of magnetic field.

(iii) Special cases are considered as motion independent of θ , motion independent on z and Motion independent of θ and z in poroelastic medium, as well as in the isotropic case for very large wave numbers and dispersion curves for longitudinal mode.

(iv) The results presented in this paper will be very helpful for researchers concerning with poroelastic materials, designers of new materials, as well as for those working on the development of a theory of hyperbolic

propagation. Study of the phenomenon of magnetic field are also used to improve the medicinal fields.

References

- Abd-Alla, A.M. and Abo-Dahab, S.M. (2013), "Effect of magnetic field on poroelastic bone model for internal remodeling", *Appl. Math. Mech.*, **34**, 889-906.
- Abd-Alla, A.M. and Yahya, G.A. (2013), "Wave propagation in a cylindrical human long wet bone", *J. Comput. Theor. Nanosci.*, **10**, 750-755.
- Abd-Alla, A.M., Abo-Dahab, S.M. and Bayones, F.S. (2015), "Wave propagation in fibre-reinforced anisotropic thermoelastic medium subjected to gravity field", *Struct. Eng. Mech.*, **53**, 277-296.
- Abd-Alla, A.M., Abo-Dahab, S.M. and Mahmoud S.R. (2011), "Wave propagation modeling in cylindrical human long wet bones with cavity", *Meccanica*, **46**, 1413-1428.
- Abo-Dahab, S.M., Abd-Alla, A.M. and Alqosami, S. (2014), "Effect of rotation on wave propagation in hollow poroelastic circular cylinder", *Math. Probl. Eng.*, **2014**, Article ID 879262, 16.
- Abo-Dahab, S.M., Abd-Alla, A.M. and Khan, A. (2016), "Rotational effect on Rayleigh, Love and Stoneley waves in non-homogeneous fibre-reinforced anisotropic general viscoelastic media of higher order", *Struct. Eng. Mech.*, **58**, 181-197.
- Ahmed, S.M. and Abd-Alla, A.M. (2002), "Electromechanical wave propagation in a cylindrical poroelastic bone with cavity", *Appl. Math. Mech.*, **133**, 257-286.
- Akbarov, S.D., Ismailov, M.I., Marin, M., Abd-Alla, A.M. and Raducanu, D. (2015), "Dynamics of the moving load acting on the hydro-elastic system consisting of the elastic plate, compressible viscous fluid and rigid wall", *CMC: Comput. Mater. Continua*, **45**(2), 75-105.
- Bakora, A. and Tounsi, A. (2015), "Thermo-mechanical post-buckling behavior off thick functionally graded plates resting on elastic foundations", *Struct. Eng. Mech.*, **56**(1), 85-106.
- Belabed, Z., Houarib, M.A., Tounsi A., Mahmoud, S.R. and Anwar, B.O. (2014), "An efficient and simple higher order shear and normal deformation theory for functionally graded material (FGM) plates", *Compos. Part B*, **60**, 274-283.
- Biot, M.A. (1955), "Theory of elasticity and consolidation for a porous anisotropic solid", *J. Appl. Phys.*, **26**(2), 182-185.
- Biot, M.A. (1956), "Theory of propagation of elastic waves in a fluid-saturated porous solid. I: low-frequency range", *Acoust. Soc. Am.*, **28**, 168-178.
- Bouderba, B., Houari, M.S.A. and Tounsi, A. (2013), "Thermomechanical bending response of FGM thick plates resting on Winkler-Pasternak elastic foundations", *Steel Compos. Struct.*, **14**(1), 85-104.
- Brynk, T., Hellmich, C., Fritsch, A., Zysset, P. and Eberhardsteiner, J. (2011), "Experimental poromechanics of trabecular bone strength: Role of Terzaghi's effective stress and of tissue level stress fluctuations", *J. Biomech.*, **44**(3), 501-508.
- Cardoso, L. and Cowin, S.C. (2012), "Role of structural anisotropy of biological tissues in poroelastic wave propagation", *Mech. Mater.*, **44**, 174-188.
- Cowin, S.C. (1999), "Bone poroelasticity", *J. Biomech.*, **32**, 217-238.
- Cui, L., Cheng, A.H.D. and Abousleiman, Y. (1997), "Poroelastic solutions of an inclined borehole", *Tran. ASME, J. Appl. Mech.*, **64**, 32-38.
- Davis Sr, C.F. (1970), "On the mechanical properties and a poroelastic theory of stress in bone", Ph.D. Thesis, University of

- Delaware.
- Ding, H. and Chenbuo, L. (1996), "General solution for coupled equations for piezoelectric Media", *Int. J. Solid. Struct.*, **16**, 2283-2298.
- El-Naggar, A.M., Abd-Alla, A.M. and Mahmoud, S.R. (2001), "Analytical solution of electro-mechanical wave propagation in long bones", *Appl. Math. Comput.*, **119**, 77-98.
- Fekrar, A., Houari, M.S.A., Tounsi, A. and Mahmoud, S.R. (2014), "A new five-unknown refined theory based on neutral surface position for bending analysis of exponential graded plates", *Meccanica*, **49**, 795- 810.
- Fl, Y.K., Houari, M.S.A. and Tounsi, A. (2014), "A refined and simple shear deformation theory for thermal buckling of solar functionally graded plates on elastic foundation", *Int. J. Comput. Meth.*, **11**(5), 135-150.
- Ghista, D.N. (1979), *Applied Physiological Mechanics*, Ellis Harwood, Chichester.
- Ghista, D.N. (1979), *Applied Physiological Mechanics*, Ellis Harwood, Chichester.
- Gilbert, R.P., Guyenne, P. and Ou, M.Y. (2012), "A quantitative ultrasound model of the bone with blood as the interstitial fluid", *Math. Comput. Model.*, **55**, 2029-2039.
- Hebali, H., Tounsi, A., Houari, M.S.A., Bessaim, A. and Bedia, E.A. (2013), "Thermoelastic bending analysis of functionally graded sandwich plates using a new higher order shear and normal deformation theory", *Int. J. Mech. Sci.*, **76**, 102-111.
- Hebali, H., Tounsi, A., Houari, M.S.A., Bessaim, A. and Bedia, E.A. (2014), "New quasi-3D hyperbolic shear deformation theory for the static and free vibration analysis of functionally graded plates", *J. Eng. Mech.*, **140**, 374-383.
- Kumar, R., Sharma, N. and Lata, P. (2016), "Effects of hall current in a transversely isotropic magnetothermoelastic with and without energy dissipation due to normal force", *Struct. Eng. Mech.*, **57**, 91-103.
- Marin, M., Abd-Alla, A.M., Raducanu, D. and Abo-Dahab, S.M. (2015), "Structural continuous dependence in micropolar porous bodies", *CMC: Comput. Mater. Continua*, **45**(2), 107-125.
- Mathieu, V. and Vayron, R. (2012), "Emmanuel soffer and fani anagnostou, influence of healing time on the ultrasonic response of the bone-implant interface", *Ultras. Med. Biology*, **38**(4), 611-618.
- Mathieu, V., Vayron, R., Richard, G., Lambert, G., Naili, S., Meningaud, J.P. and Haiat, G. (2014), "Biomechanical determinants of the stability of dental implants: Influence of the bone-implant interface properties", *J. Biomech.*, **47**(1), 3-13.
- Matuszyk, P.J. and Demkowicz, L.F. (2014), "Solution of coupled poroelastic/acoustic/elastic wave propagation problems using automatic hp-", *Comput. Meth. Appl. Mech. Adapt. Eng.*, **281**, 54-80.
- Meziane, M.A.A., Henni, A.H. and Tounsi, A. (2014), "An efficient and simple refined theory for buckling and free vibration of exponentially graded sandwich plates under various boundary conditions", *J. Sandw. Struct. Mater.*, **16**(3), 293- 318.
- Misra, J.C. and Samanta, S.C. (1984), "Wave propagation in tubular bones", *Int. J. Solid. Struct.*, **20**(1), 55-62.
- Misra, J.C., Chatopadhyay, N.C. and Samanta, S.C. (1994), "Thermo-viscoelastic waves in an infinite aeolo-tropic body with a cylindrical cavity a study under the review of generalized theory of thermoelasticity", *Compos. Struct.*, **52**(4), 705-717.
- Morin, C. and Hellmich, C. (2014), "A multiscale poromicromechanical approach to wave propagation and attenuation in bone", *Ultrasonics*, **54**, 1251-1269.
- Natal, A.N. and Meroi, E.A. (1986), "A review of the biomechanical properties of bone as a material", *J. Biomed. Eng.*, **11**, 266-277.
- Nguyen, V.H., Lemaire, T. and Naili, S. (2010), "Poroelastic behaviour of cortical bone under harmonic axial loading: A finite element study at the osteonal scale", *Med. Eng. Phys.*, **32**(4), 384-390.
- Papathanasopoulou, V.A., Fotiadis, D.I., Foutsitzi, G. and Massalas, C.V. (2002), "A poroelastic bone model for internal remodeling", *Int. J. Eng. Sci.*, **40**(5), 511-530.
- Parnell, W.J., Vu, M.B., Grimal, Q. and Naili, S. (2012), "Analytical methods to determine the effective mesoscopic and macroscopic elastic properties of cortical bone", *Biomech. Model. Mechanobio.*, **11**(6), 883-901.
- Potsika, V.T., Grivas, K.N., Protopappas, V.C., Vavva, M.G., Raum, K., Rohrbach, D., Polyzos, D. and Fotiadis, D.I. (2014), "Application of an effective medium theory for modeling ultrasound wave propagation in healing long bones", *Ultrasonics*, **54**(5), 1219-1230.
- Qin, Q.H., Qu, C. and Ye, J. (2005), "Thermoelectroelastic solutions for surface bone remodeling under axial and transverse loads", *Biomater.*, **26**(3), 6798-6810.
- Said, S.M. and Othman, M.I.A. (2016), "Wave propagation in a two-temperature fiber-reinforced magento-thermoelastic medium with tgree-phase-lag model", *Struct. Eng. Mech.*, **57**, 201- 220.
- Shah, S.A. (2008), "Axially symmetric vibrations of fluid-filled poroelastic circular cylindrical shells", *Journal of Sound and Vibration*, **318**, 389-405.
- Shah, S.A. (2011), "Flexural wave propagation in coated poroelastic cylinders with reference to fretting fatigue", *J. Vib. Control*, **17**, 1049-1064.
- Tounsi, A. (2013), "A refined trigonometric shear deformation theory for thermoelastic bending of functionally graded sandwich plates", *Aerosp. Sci. Technol.*, **24**, 209- 220.
- Wen, P.H. (2010), "Meshless local Petro-Galerkin (MLPG) method for wave propagation in 3D porolastic solids", *Eng. Anal. Bound. Elem.*, **34**, 315-323.
- Zidi, M., Tounsi, A., Houari, M.S.A., Bedia, A., Anwar, E.A. and Bég, O. (2014), "Bending analysis of FGM plates under hygro-thermo-mechanical loading using a four variable refined plate theory", *Aerosp. Sci. Technol.*, **34**, 24-34.

CC

$$a_{43} = \left(\bar{M} - \frac{\dot{Q}e_3}{k^2} + \frac{\dot{K}e_3}{k^2} \right) \left[\left(\frac{n^2}{\alpha_3^2 \bar{a}^2} - \frac{n^2}{\bar{a}^2} - 1 \right) J_n(\alpha_3 \bar{a}) \right. \\ \left. + \left(\frac{1}{\alpha_3 \bar{a}} - \frac{1}{\bar{a}} \right) J_{n+1}(\alpha_3 \bar{a}) \right]$$

$$a_{44} = 0, \dots$$

$$a_{45} = \left(\bar{M} - \frac{\dot{Q}e_1}{k^2} + \frac{\dot{K}e_1}{k^2} \right) \left[\left(\frac{n^2}{\alpha_1^2 \bar{a}^2} - \frac{n^2}{\bar{a}^2} - 1 \right) Y_n(\alpha_1 \bar{a}) \right. \\ \left. + \left(\frac{1}{\alpha_1 \bar{a}} - \frac{1}{\bar{a}} \right) Y_{n+1}(\alpha_1 \bar{a}) \right]$$

$$a_{46} = \left(\bar{M} - \frac{\dot{Q}e_2}{k^2} + \frac{\dot{K}e_2}{k^2} \right) \left[\left(\frac{n^2}{\alpha_2^2 \bar{a}^2} - \frac{n^2}{\bar{a}^2} - 1 \right) Y_n(\alpha_2 \bar{a}) \right. \\ \left. + \left(\frac{1}{\alpha_2 \bar{a}} - \frac{1}{\bar{a}} \right) Y_{n+1}(\alpha_2 \bar{a}) \right]$$

$$a_{47} = \left(\bar{M} - \frac{\dot{Q}e_3}{k^2} + \frac{\dot{K}e_3}{k^2} \right) \left[\left(\frac{n^2}{\alpha_3^2 \bar{a}^2} - \frac{n^2}{\bar{a}^2} - 1 \right) Y_n(\alpha_3 \bar{a}) \right. \\ \left. + \left(\frac{1}{\alpha_3 \bar{a}} - \frac{1}{\bar{a}} \right) Y_{n+1}(\alpha_3 \bar{a}) \right]$$

$$a_{48} = 0 ,$$

The remaining four can be obtained from the above equations by replacing \bar{a} by \bar{b}